

# Crossreactive T Cells Spotlight the Germline Rules for $\alpha\beta$ T Cell-Receptor Interactions with MHC Molecules

Shaodong Dai,<sup>1,2</sup> Eric S. Huseby,<sup>1,2,5</sup> Kira Rubtsova,<sup>2</sup> James Scott-Browne,<sup>2</sup> Frances Crawford,<sup>1,2</sup> Whitney A. Macdonald,<sup>6</sup> Philippa Marrack,<sup>1,2,3,\*</sup> and John W. Kappler<sup>1,2,4</sup>

<sup>1</sup>Howard Hughes Medical Institute and

<sup>2</sup>Integrated Department of Immunology

National Jewish Medical and Research Center, Denver, CO 80206, USA

<sup>3</sup>Department of Biochemistry and Molecular Genetics, University of Colorado at Denver and Health Sciences Center, Aurora, CO 80045, USA

<sup>4</sup>Program in Biomolecular Structure, University of Colorado at Denver and Health Sciences Center, Aurora, CO 80045, USA

<sup>5</sup>Present address: Department of Pathology, University of Massachusetts Medical School, Worcester, MA 01605, USA.

<sup>6</sup>Present address: Department of Biochemistry and Molecular Biology, School of Biomedical Sciences, Monash University, Clayton, Victoria 3800, Australia.

\*Correspondence: [marrackp@njc.org](mailto:marrackp@njc.org)

DOI 10.1016/j.immuni.2008.01.008

## SUMMARY

To test whether highly crossreactive  $\alpha\beta$  T cell receptors (TCRs) produced during limited negative selection best illustrate evolutionarily conserved interactions between TCR and major histocompatibility complex (MHC) molecules, we solved the structures of three TCRs bound to the same MHC II peptide (IA<sup>b</sup>-3K). The TCRs had similar affinities for IA<sup>b</sup>-3K but varied from noncrossreactive to extremely crossreactive with other peptides and MHCs. Crossreactivity correlated with a shrinking, increasingly hydrophobic TCR-ligand interface, involving fewer TCR amino acids. A few CDR1 and CDR2 amino acids dominated the most crossreactive TCR interface with MHC, including V $\beta$ 8 48Y and 54E and V $\alpha$ 4 29Y, arranged to impose the familiar diagonal orientation of TCR on MHC. These interactions contribute to MHC binding by other TCRs using related V regions, but not usually so dominantly. These data show that crossreactive TCRs can spotlight the evolutionarily conserved features of TCR-MHC interactions and that these interactions impose the diagonal docking of TCRs on MHC.

## INTRODUCTION

$\alpha\beta$  T cell receptors (TCRs) are created by rearrangements of germline V, D, and J genes and nongermline-encoded CDR3 segments during thymocyte development. The collection of TCRs thus produced is culled by positive and negative selection in the thymus to establish the mature TCR repertoire. Positive selection picks out for survival thymocytes bearing TCRs that react weakly with MHC peptides in the thymus (Hogquist et al., 1994; Sebзда et al., 1994; Sprent et al., 1988). Negative selection destroys thymocytes with TCRs that engage self-MHC-self-pep-

tide ligands too strongly (Bluthmann et al., 1988; Kappler et al., 1987). The surviving cells constitute the mature T cell population, whose TCR affinities and/or avidities for self-MHC-self-peptides are too low for T cell activation, thus avoiding autoimmunity. However, replacement of the self-peptide with a foreign peptide converts the complex into a high-affinity ligand for some of the T cells, thereby leading to successful immune responses.

We still do not understand how TCRs react nearly exclusively with MHC ligands. The evolutionary hypothesis suggests that TCR genes have evolved to encode proteins that are inherently MHC specific (Jerne, 1971). Alternatively, the initial TCR repertoire may be random, and positive selection may pick out the rare TCRs with the appropriate MHC specificity and affinity.

We have studied T cells in mice expressing an MHC class II (MHC II) with a single covalently bound peptide that excludes the binding of other peptides, including self-peptides (Huseby et al., 2005; Ignatowicz et al., 1996). These mice have a substantial mature CD4<sup>+</sup> T cell repertoire. However, many of these T cells have unusual specificities. Most react with the wild-type form of the same MHC II molecule with the normal contingent of self-peptides. Many also react with many other MHC II alleles (Fung-Leung et al., 1996; Huseby et al., 2003; Ignatowicz et al., 1996; Martin et al., 1996; Miyazaki et al., 1996) and even cross-react with MHC I ligands (Huseby et al., 2005). Immunization of these mice with the same MHC II bound to a foreign peptide produces MHC-peptide-reactive T cells that are also self- and allo-MHC reactive and also tolerate many mutations of their MHC-II-foreign-peptide ligand.

These results led us to propose a variant of the evolutionary hypothesis. We suggested that in normal animals, the CDR1 and CDR2 loops of germline-encoded TCR V elements produce MHC-crossreactive T cells with high frequency. These T cells can be positively selected, but their likelihood of survival is dependent on the somatically generated V region CDR3 loops, which must attenuate the conserved MHC interactions in order for the T cell bearing them to escape negative selection. The many self-MHC-self-peptides combinations in the thymuses of normal mice make escape difficult, because at least some

combinations are likely to permit enough of the conserved MHC interaction to drive negative selection. However, the single MHC peptide present in our mice allows many of these normally deleted crossreactive T cells to avoid negative selection and appear in the mature T cell population (Huseby et al., 2005).

We reasoned that this highly crossreactive population of T cells provides a unique opportunity to look for TCRs manifesting relatively unadulterated examples of germline TCR-MHC interactions. Therefore, we solved the structures of three TCRs bound to the same MHC II molecule, IA<sup>b</sup>, occupied by the same peptide, 3K. One TCR was from a highly MHC-peptide-specific T cell, B3K506, isolated from normal C57BL-6 mice (Huseby et al., 2005; Rees et al., 1999). The other two TCRs were from T cells isolated from IA<sup>b</sup> single-peptide mice (Huseby et al., 2005). One of these (2W20) was modestly crossreactive, and the other (Yae62) was extremely crossreactive. All three TCRs used members of the mouse V $\beta$ 8 (BV8) family, and two (B3K506 and Yae62) used members of the V $\alpha$ 4 family (Arden et al., 1995).

The footprints of the TCRs on IA<sup>b</sup>-3K were very different ranging from a large, nonhydrophobic interaction for the highly specific TCR to a much smaller, hydrophobic interaction for the highly crossreactive TCR. As predicted by our hypothesis, interactions involving the TCR germline CDR1 and CDR2 regions became highly focused on just a few TCR amino acids as the TCR progressed from highly specific to highly crossreactive. These included two amino acids, V $\beta$ 8 46Y and 48Y, which others have suggested might mediate conserved MHC interactions (Feng et al., 2007), and V $\beta$ 8 54E, as well as V $\alpha$ 4 29Y, previously unnoticed as a potentially conserved MHC-interacting amino acid. These V $\alpha$  and V $\beta$  amino acids and their binding sites on MHC impose a diagonal mode of docking for TCR on MHC. These results explain how crossreactive TCRs might operate and support our hypothesis that these TCRs may be good tools for identification of the features of TCR V regions that predispose them to MHC reactivity.

## RESULTS

### Structures of the Complexes of Three TCRs Bound to the Same MHC Peptide

The complexes of soluble versions of the highly specific, B3K506, moderately crossreactive, 2W20, and highly crossreactive, Yae62, TCRs bound to the IA<sup>b</sup>-3K ligand were expressed, crystallized, and solved to resolutions of 2.55 Å, 3.40 Å and 3.05 Å, respectively (Table S1 and Figure S1 available online). Viewed from the T cell (Figures 1A–1C), the six CDR regions of all three TCRs lie in the now familiar diagonal configuration over the MHC-II-peptide complex with the V $\beta$  domains of the TCRs over the IA<sup>b</sup>  $\alpha$ 1 helix and the V $\alpha$  domains over the  $\beta$ 1 helix (Garboczi et al., 1996; Garcia et al., 1996). The angle of this orientation ( $\sim 45^\circ$  to the peptide backbone) is very similar for all three TCRs. However, a view from the N-terminal end of the 3K peptide (Figures 1D–1F) shows that the B3K506 TCR engages the MHC peptide tilted somewhat to the MHC  $\beta$  chain helix, whereas the 2W20 TCR is tilted more and the Yae62 TCR even more toward the MHC  $\alpha$  chain helix.

These differences in tilt and in the compositions of the CDR3s of the TCRs lead to very different footprints of the TCRs on

IA<sup>b</sup>-3K (Figures 2A–2C, Table 1, and Spreadsheet S1). The B3K506 TCR interacts extensively with both the MHC and peptide. The result is a large, distributed footprint with a buried surface of 1893 Å<sup>2</sup>, typical of that seen in most other TCR:MHC-peptide structures (Rudolph et al., 2006). The 2W20 TCR interacts with fewer MHC and peptide atoms for a footprint of 1695 Å<sup>2</sup>, and the Yae62 TCR contacts even fewer MHC and peptide atoms for a footprint of only 1178 Å<sup>2</sup>, the smallest yet reported for a TCR in complex with classical MHC.

### Interpreting IA<sup>b</sup>-3K Mutational Studies on the Basis of the Structures

The observed footprints of these TCRs correlate well with the results of extensive mutagenesis studies of their interaction with their MHC-peptide ligand (Huseby et al., 2006; Huseby et al., 2005). In these studies, the five most exposed amino acids of the  $\alpha$ 1 helix (55D, 57Q, 61Q, 64A, and 68H),  $\beta$ 1 helix (66E, 70R, 73A, 77T, and 81H), and the peptide (–1E, 2Q, 3K, 5K, and 8K) of IA<sup>b</sup>-3K were mutated to many other amino acids. We assessed the effects of the mutations on their interaction with the three TCRs, as judged by T cell hybridoma activation and by TCR binding to IA<sup>b</sup>-3K and its mutants, measured by flow cytometry and surface-plasmon resonance.

For the most part, those amino acids whose mutation had the greatest effect in these assays were also those that contributed the most to the footprint of the IA<sup>b</sup>-3K on the TCRs in the X-ray crystal structures, as illustrated in Figures 2D–2F, which show the number of atom-to-atom contacts each of the engaged amino acids of IA<sup>b</sup>-3K makes with the TCRs in the three structures. Clearly, some MHC amino acids, for example IA<sup>b</sup>  $\alpha$ 57Q and  $\alpha$ 61Q, are heavily engaged by all three TCRs, whereas others, for example IA<sup>b</sup>  $\alpha$ 68H, are less involved. In these figures, the 13 amino acids that were involved in our mutagenesis studies and that were not alanine are boxed to reflect the effect on TCR-binding energy of their mutation to alanine, i.e., removal of their side chain. A green box indicates a  $\Delta\Delta G$  increase of  $\leq 0.8$  kcal-mole ( $\leq \sim 75\%$  loss of affinity), and a red box indicates a  $\Delta\Delta G$  increase of  $> 0.8$  kcal-mole. As a first approximation, we can view these measurements as reflecting the contribution of the amino acid side-chain atoms after the C $\beta$  carbon to the binding affinity, but secondary effects, such as repositioning of adjacent amino acids or changes in structured water within the interface, cannot be ruled out.

Our findings show that, for all three TCRs, all 26 amino acids whose mutation to A resulted in a  $\Delta\Delta G$  increase of  $> 0.8$  kcal-mole made at least three contacts with the relevant TCR in the solved structures (Figure 3). Moreover, for each of the IA<sup>b</sup>  $\alpha$  chain, IA<sup>b</sup>  $\beta$  chain, and peptide portions of the ligand, mutation of the amino acid with the most TCR contacts invariably increased  $\Delta\Delta G > 0.8$  kcal-mole. For the remaining 13 amino acids, mutation to A did not dramatically reduce the affinity of TCR binding. In the structures, these were either not in contact with the TCR or were at the edges of the footprint where the binding of their side-chain binding might be predicted to be less important.

Our mutational experiments also identified “interface disrupting amino acids,” amino acids that were either A to begin with or whose mutation to A did not dramatically reduce TCR binding, but whose mutation to a number of other amino acids inhibited binding (Huseby et al., 2006; Huseby et al., 2005). For example,

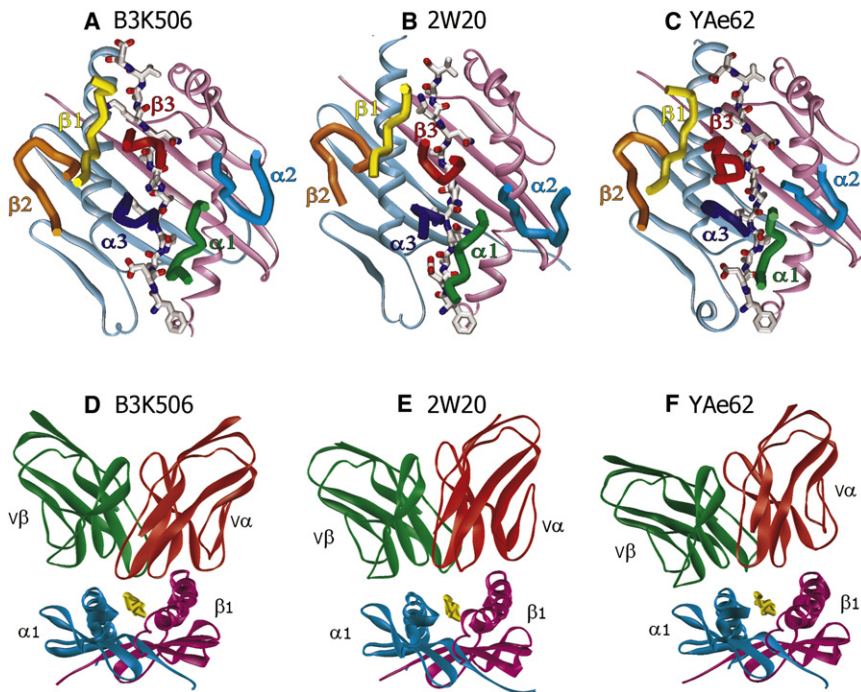


**Figure 1. Orientation of the TCRs on Their  $IA^b$ -3K Ligand**

For the (A) B3K506, (B) 2W20, and (C) YAe62 TCRs bound to  $IA^b$ -3K, a top view of the  $IA^b$   $\alpha 1$  and  $\beta 1$  domains are shown as ribbons colored light cyan and light magenta, respectively, with the bound 3K peptide shown as a wireframe with CPK coloring. For each complex the six TCR CDR loops are shown as tubes colored as follows:  $\alpha$ CDR1, green;  $\alpha$ CDR2, dark cyan;  $\alpha$ CDR3, blue;  $\beta$ CDR1, yellow;  $\beta$ CDR2, orange;  $\beta$ CDR3, red. For the (D) B3K506, (E) 2W20, and (F) YAe62 TCRs bound to  $IA^b$ -3K, views are shown looking down the  $IA^b$  peptide-binding groove from the peptide N terminus. Ribbon representations of the  $IA^b$   $\alpha 1$  and  $\beta 1$  domains (cyan and magenta, respectively) and TCR  $V\alpha$  and  $V\beta$  domains (red and green) are shown. The 3K peptide is represented with a yellow tube.

$IA^b$   $\alpha 64A$  in all three structures and  $IA^b$   $\beta 73A$  in the B3K506 and 2W20 structures lie within the TCR footprint but are not major sites of contact. In each case, we identified other amino acids that, when substituted for the A, strongly inhibited TCR binding ( $\Delta\Delta G$  increases of  $>0.8$  kcal-mole) and/or T cell activation. The most straight-forward structural interpretation of these results is that steric interference by the side chains of these mutated amino acids disrupted TCR binding. Other examples were amino acids at the periphery of the TCR footprints, e.g.,  $IA^b$   $\alpha 55D$  and  $\alpha 68H$ , where mutation to A had a minimal effect, but mutation to numerous other amino acids disrupted TCR binding. Again, steric interference is the most straight-forward interpretation of these results.

### The Nature of the TCR-MHC Interface in Relation to TCR Crossreactivity

The three TCRs in this study bind to their  $IA^b$ -3K ligand with very similar affinities ( $\sim 10$   $\mu M$ ) and binding kinetics (Huseby et al., 2006). Our mutational analyses showed that changing the side chains of many of the exposed surface MHC and peptide amino acids had much less effect on the crossreactive T cells than on highly specific ones. To explain this result in light of the similar TCR affinities, we suggested that perhaps the crossreactive T cells maintained affinity by making fewer contacts with the  $IA^b$ -3K amino acid side chains and more contacts with the MHC and peptide backbone, thus preserving a similar area of contact while becoming less susceptible to mutations. However, the structures of the three complexes show that this suggestion was not correct. In fact, as described above, the mutational data quite accurately predicted the decreasing size of the three TCR footprints as the TCR became more crossreactive (Figure 2).

Affinity can be preserved, even though the surface area of interaction is reduced, if the chemical nature of the interfaces

between the TCRs and  $IA^b$ -3K ligands is different between the noncrossreactive and crossreactive TCRs. To check this, we analyzed the details of the TCR-MHC interfaces in the three complexes (Table 1 and Spreadsheet S1). Not unexpectedly, there is a direct relationship between the decreasing size of the TCR footprint and the total number of MHC-peptide atoms contacted as one proceeds from the most specific (B3K506) to the most crossreactive (YAe62) TCR. Also, as the TCR tips further toward the MHC  $\alpha$  chain, there are more MHC  $\alpha$  chain atoms and fewer MHC  $\beta$  chain atoms contacted. Finally, the ratio of MHC to peptide atoms involved in the interface changes dramatically between the most specific and most crossreactive TCR. Thus, the TCR footprint shrinks and focuses more on the MHC than on the peptide as crossreactivity increases. However, despite the smaller footprint involving few ligand atoms, the total number of atom-to-atom contacts does not decrease dramatically with increasing crossreactivity. Thus, there are more TCR contacts per ligand atom.

Perhaps the most striking difference among the TCR interfaces is the relative ratio of the various types of atom-to-atom contacts. For B3K506,  $\sim 1/4$  of the interactions are C to C van der Waals (VDW) in nature, for 2W20,  $\sim 1/3$ , and for YAe62,  $\sim 1/2$  (Table 1). Aromatic amino acids (Y, F, and W) play a large role in the hydrophobic nature of the crossreactive TCR footprints (Spreadsheet S1). Particularly noteworthy are the  $V\beta$  CDR3s of the 2W20 and YAe62 TCRs, in which a W and an F make major contributions to the interface.

Although individual VDW interactions are weak, a concentrated area of C-to-C hydrophobic interaction, such as is often found in the cores of globular proteins or in protein subunit interfaces, can be very stabilizing because of the "hydrophobic effect." These observations lead us to propose that T cells become highly crossreactive via a concentrated hydrophobic interface that focuses on the MHC portion of the ligand but with a minimal area of contact. This allows the receptor to maintain high-affinity binding and to be tolerant to changes in many of the amino acids of the peptide and the rest of the MHC surface.

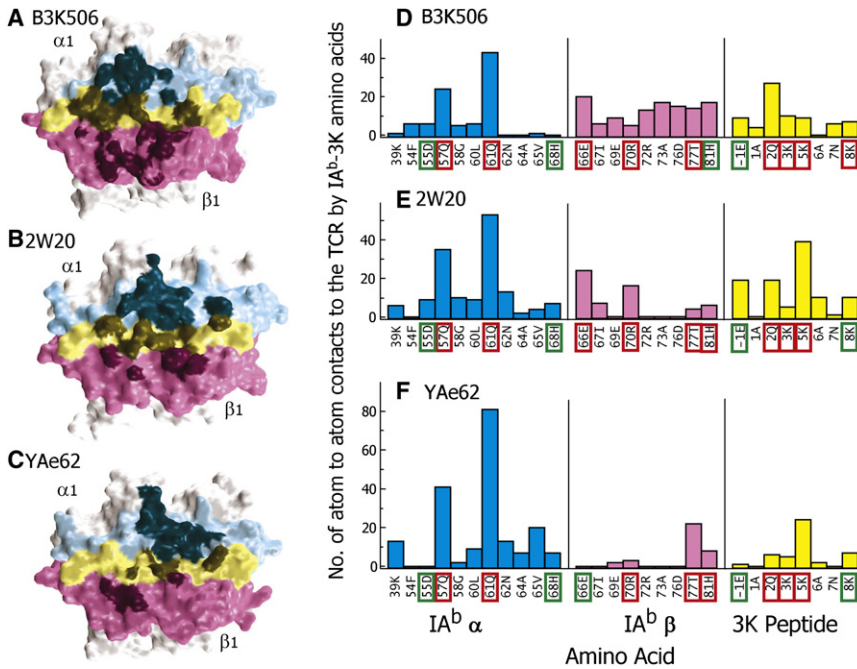


**Figure 2. The Footprint of the TCRs on IA<sup>b</sup>-3K**

In the first three panels, the areas of contact on the IA<sup>b</sup>-3K ligand are shown for the (A) B3K506, (B) 2W20, and (C) YAE62 TCRs. In each case, the water-accessible surface of the  $\alpha 1$ - $\beta 1$ -peptide portions of IA<sup>b</sup>-3K is shown, viewed looking directly at the areas of TCR contact. The portion of the IA<sup>b</sup>-3K surface in contact with the TCRs is colored as follows: that from atoms in  $\alpha 1$ , dark cyan; from  $\beta 1$ , dark magenta; and from the peptide, dark yellow. The rest of the surface is colored as follows:  $\alpha 1$  helix, light cyan;  $\beta 1$  helix, light magenta; peptide light yellow; and the rest of  $\alpha 1$  and  $\beta 1$ , white. In the second three panels, the number of atom-to-atom contacts between the (D) B3K506, (E) 2W20, or (F) YAE62 TCR and individual IA<sup>b</sup>-3K amino acids within the  $\alpha$  chain (cyan),  $\beta$  chain (magenta) and peptide (yellow) portion of the ligand is shown. Data are shown for all IA<sup>b</sup>-3K amino acids that contact the TCR in any of the structures. The IA<sup>b</sup>-3K nonalanine amino acids that were previously (Huseby et al., 2006) subjected to mutational analysis are highlighted with a rectangle. A green rectangle indicates that when this position was mutated to alanine and tested for TCR binding, there was an increase in  $\Delta\Delta G$  of  $\leq 0.8$  kcal-mole. A red rectangle indicates an increase of  $>0.8$  kcal-mole.

### Conserved TCR Interactions with MHC Are Used by the Crossreactive TCR

We have hypothesized that the evolutionarily conserved interactions between TCRs and MHC, were they to exist, might best be demonstrated best by very crossreactive TCRs that have been through limited negative selection (Huseby et al., 2005). With this in mind, we determined the number of atom-to-atom contacts individual amino acids of the TCR made with the IA<sup>b</sup> portion of the ligand (Figure 3 and Spreadsheet S1). In all three structures, the CDR3 regions of V $\alpha$  and/or V $\beta$  contribute to the interface. However, we confined the analysis to V $\alpha$  and V $\beta$  CDR1 and CDR2 because, although partially constructed from germline-encoded amino acids, the extreme somatic variability in the composition and length in the CDR3 loops would seem to exclude the germline maintenance of any specific conserved interactions.

Because the highly specific B3K506 and highly crossreactive YAE62 TCRs both use related members of the V $\alpha 4$  and V $\beta 8$  families, their comparison was particularly informative. The CDR1-CDR2 interface of the YAE62 TCR with IA<sup>b</sup> was dominated by just three amino acids, V $\alpha$  29Y, V $\beta$  48Y, and V $\beta$  54E, which account for 85% of the total CDR1-CDR2 contacts (Figure 3C). These amino acids were present in the B3K506 TCR interface as well, but they were less predominant there because of contributions from many other amino acids (Figure 3A). The intermediately crossreactive 2W20 TCR also uses a member of the V $\beta 8$  family, whose 48Y and 54E also contributed substantially more to the interface than seen in the B3K506 structure (Figure 3B). Moreover, as discussed further below, consistent interactions with MHC by V $\beta$  48Y and V $\beta$  54E have been noted before by others (Feng et al., 2007; Maynard et al., 2005). The 2W20 TCR contained a member of the V $\alpha 2$  rather than V $\alpha 4$  family. However,

the V $\alpha$  CDR1 loop of the 2W20 also makes contact with the IA<sup>b</sup> portion of the ligand via two amino acids, 27S and 30D.

Our hypothesis leads us to propose that these amino acids are conserved features of these V elements used for MHC recognition. If this idea is correct, these amino acids should be interacting with conserved sites on the MHC II molecule. Figure 4 shows that in the three structures, the V $\alpha$  CDR1s do indeed interact similarly with a highly conserved site on the IA<sup>b</sup>  $\beta$  chain. For example, in both the B3K506 and YAE62 structures, 29Y extends from the tip of V $\alpha$  CDR1 and inserts between the side chains of 77T and 81H on the IA<sup>b</sup>  $\beta$  chain  $\alpha$  helix (Figures 4A and 4C). In the case of the B3K506 TCR, the tilt of the receptor toward the  $\beta$  chain side of the IA<sup>b</sup> has pushed 29Y over the edge of the helix to interact with  $\beta 76D$  as well.  $\beta 76D$  and  $\beta 81H$  are nearly invariant in mouse and human MHC II molecules, whereas  $\beta 77T$  is the most commonly found amino acid at this position (Lefranc et al., 2003). 27S and 30D of the 2W20 V $\alpha$  CDR1 loop and interact with the same region of the  $\beta$  chain, thus contacting IA<sup>b</sup>  $\beta 81H$  and  $\beta 77T$  (Figure 4B). Although the extent of contact with these two amino acids is not as great as seen with V $\alpha$  Y29 in the YAE62 structure, mutation of either  $\beta 81H$  or  $\beta 77T$  to alanine in our mutational studies severely reduced 2W20 interaction with IA<sup>b</sup>-3K (Figure 3B).

Similarly, V $\beta$  48Y and 54E also interact with a conserved target site on the MHC  $\alpha$  chain (Figures 4D–4F). In all three structures, V $\beta$  48Y is nestled among the side chains of three amino acids on the IA<sup>b</sup>  $\alpha$  chain  $\alpha$  helix: 57Q, 60L, and 61Q. The ability of this region of the CDR2 loop of V $\beta$  to approach the helix is facilitated by the lack of a sterically hindering side chain at IA<sup>b</sup>  $\alpha$  64A. 57Q, 60L, and 64A are nearly invariant in MHC II molecules, and 61Q is the most frequent amino acid at this position. In the 2W20 and YAE62 structures, V $\alpha$  54E also contacts this area of the  $\alpha$  chain  $\alpha$  helix, and thus interacts with 57Q and 60L, but it also makes

**Table 1. Characterization of the TCR Interfaces with IA<sup>b</sup>-3K**

	B3K506	2W20	YAE
Footprint (Å <sup>2</sup> )	1893	1695	1178
No. of Ligand Atoms Contacted			
MHC $\alpha$	29	46	46
MHC $\beta$	44	23	12
Peptide	34	27	16
Total	107	96	74
Ratio (MHC/Peptide)	2.2	2.5	3.6
Atom-to-Atom Contacts			
C to C VDW	67	102	136
Other VDW	192	186	130
H bonds or Salt Bridges	21	20	7
Total Contacts	280	308	273
Contacts per Ligand Atom	2.6	3.2	3.6
Proportion C to C (%)	24	33	50

a number of contacts with 39K, including a salt bridge. 39K sits on the  $\alpha$  chain loop connecting the third and fourth beta strands and is highly conserved in mouse IA and human DR molecules (Lefranc et al., 2003). The tilt of the B3K506 TCR toward the IA<sup>b</sup>  $\beta$  chain pulls V $\beta$  54E away from the  $\alpha$  chain  $\alpha$  helix and eliminates some of its contacts, including the salt bridge to  $\alpha$  39K.

V $\alpha$  29Y is present in the CDR1 regions of ~10% of mouse V $\alpha$ s and two human V $\alpha$ s (V $\alpha$ 22 and V $\alpha$ 31). V $\alpha$  27S and 30D (or N) are found in CDR1 of the large mouse V $\alpha$ 2 family, as well as the human V $\alpha$ 8, V $\alpha$ 14, and V $\alpha$ 21 families. V $\beta$ CDR2 Y48 and E54 are present in CDR2 in 35% and 10% of mouse and human V $\beta$ s, respectively. Therefore, these amino acids are fairly well represented in the overall mouse and human V repertoire. If our hypothesis is correct, the types of interactions that we see for these amino acids in our structures should also be present to varying degrees in other mouse and human structures with one of these V regions. Therefore, we examined five published TCR-MHC II structures that contained these amino acids for the number of contacts of CDR1-CDR2 with the MHC II molecule (Figure 5).

In all of these structures, V $\alpha$  29Y or V $\alpha$  27S and 30D and V $\beta$  48Y and 54E, when present, contribute to the TCR CDR1-CDR2 interface with MHC II, interacting with the same target sites on MHC II shown in Figure 4. However, in most of these other cases, more other amino acids contributed to the interface than in the YAE62 and/or 2W20 TCR complexes. This was especially true for V $\alpha$  29Y and V $\beta$  48Y and 54E. For example, Figures 5A and 5B show the data for two TCR-MHC II structures that contain V $\alpha$  29Y, one from a human TCR using V $\alpha$ 22 (Li et al., 2005) and one from a mouse TCR using V $\alpha$ 4.9 (Feng et al., 2007). In both cases, V $\alpha$  29Y interacts with the MHC  $\beta$  chain in the same area as seen with the YAE62 and B3K506 TCRs. In the human structure, V $\alpha$  29Y is very dominant for V $\alpha$  interaction, but many V $\beta$  amino acids also contribute to the total interface. In the mouse V $\alpha$ 4.9 structure, V $\alpha$  29Y is even less predominant in the overall contacts. As far as the V $\alpha$  27S- and 30D-containing TCRs are concerned, in the other structures with TCRs containing members of the mouse V $\alpha$ 2 family, CDR1 27S and 30D are

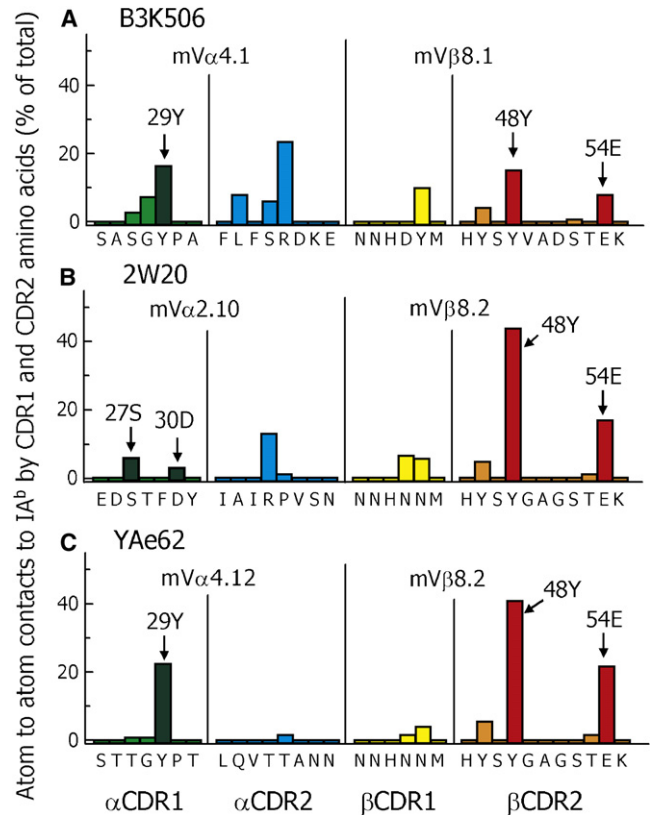


**Figure 3. Crossreactive TCRs Use Only a Few Amino Acids in CDR1-CDR2 to Bind IA<sup>b</sup>-3K**

For the (A) B3K506, (B) 2W20, and (C) YAE62 TCRs, the atom-to-atom contacts between the CDR1 and CDR2 regions of the TCR V $\alpha$  and V $\beta$  chains and IA<sup>b</sup> were calculated as described in the Experimental Procedures. The data are shown as the percentage of the total CDR1-CDR2 contacts contributed by each TCR amino acid. The sequences of the CDRs are shown with the contact data for each amino acid presented as the percentage of the total V $\alpha$ -V $\beta$  CDR1-CDR2 contacts. Bars are colored green (V $\alpha$  CDR1), cyan (V $\alpha$  CDR2), yellow (V $\beta$  CDR1), and orange (V $\beta$  CDR2), except that the bar for V $\alpha$  29Y (A and C) or 27S-30D (B) are colored dark green and the bars for V $\beta$  48Y and 54E (A, B, and C) are colored red. In each panel, the V $\alpha$  and V $\beta$  element used by the TCR is indicated.

part of the contact interface, again interacting with target sites on the MHC I  $\beta$  chain that are similar to those seen by the 2W20 TCR (Figures 4B, 5C, and 5D).

Perhaps because mouse and human V $\beta$  elements related to mouse V $\beta$ 8 make TCRs particularly amenable to expression in a soluble form, the published structures of TCRs bound to MHC I and MHC II ligands are heavily skewed toward TCR with these V $\beta$ s. Garcia and colleagues have concentrated on the analysis of these structures from their own and other laboratories (Feng et al., 2007; Maynard et al., 2005). They pointed out that V $\beta$  46Y, 48Y, and 54E (48Y, 50Y, and 56E by their number scheme) are repeatedly found in the interface between TCR and MHC II and may represent germline-encoded conserved sites of MHC interaction. Figures 5B-5E show an analysis of four TCR-MHC II published structures that contain V $\beta$  48Y and 54E, three from mouse (V $\beta$  8.2) and one from human (V $\beta$  3.1). As pointed out by Feng et al. (2007), in each structure V $\beta$  48Y

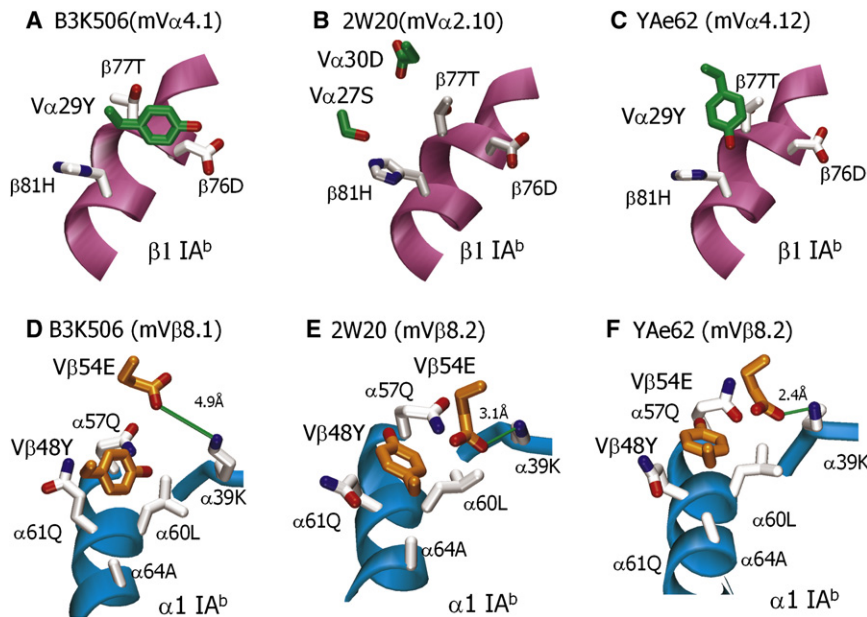


**Figure 4. V $\alpha$  29Y and V $\beta$  48Y and 54E Interact with Conserved Sites on MHC II**

The sites of interaction of the V $\alpha$  CDR1 loop with the IA<sup>b</sup>  $\beta$  chain helix is shown for the (A) B3K506, (B) 2W20, and (C) YAe62 TCRs. A stick representation of the side chain of V $\alpha$  CDR1 29Y (A and C) and 27S-30D (B) is shown (carbon is colored green, and oxygen is colored red) with a ribbon representation of a portion of the IA<sup>b</sup>  $\beta$  chain helix (magenta) and stick representations of the side chains of the relevant IA<sup>b</sup> amino acids (CPK coloring). Similarly, the sites of interaction of V $\beta$  48Y and 54E with the IA<sup>b</sup>  $\alpha$  chain is shown for the (D) B3K506, (E) 2W20, and (F) YAe62 TCRs. Stick representations of the side chains of V $\alpha$  48Y and 54E are shown (carbon is colored orange, and oxygen is colored red) with a ribbon representation of a portion of the IA<sup>b</sup>  $\alpha$  chain helix, a tube representation of a portion of the loop connecting the third and fourth  $\beta$  strands of the  $\alpha$  chain (cyan), and a stick representation of the side chains of the relevant IA<sup>b</sup> amino acids (CPK coloring).

contributes to the TCR-MHC II interface, binding to the same positions on the MHC  $\alpha$  chain helix as in Figure 4. However, again, in each of these structures many other amino acids contribute to the total interface. Another amino acid noted by Feng et al., V $\beta$  46Y, also makes contact with the MHC  $\beta$  chain helix in all of the TCR structures in which it is present, but in these structures, the overall contribution in every case is less than seen for Y48. V $\beta$  54E also makes many contacts in all the structures analyzed in Figure 5; however, this amino acid received less attention in previous analyses, perhaps because it is less consistently used in interactions between TCRs and MHC I versus with MHC II.

A picture emerges from the sum of our and these previously reported structures of a gradient of contributions from these amino acids to the CDR1-CDR2 interface with MHC II ranging from a minimum contribution in the B3K506 and HA1.7 structures to a maximum in the YAe62 structure. This gradient is consistent with our hypothesis that negative selection in the normal thymus operates to lessen the contribution from these conserved amino acids to avoid autoimmunity.

#### The Predicted Conserved Interactions between TCRs and MHC Impose the Diagonal Docking of TCRs on MHC

One of the strongest arguments in favor of the evolutionary hypothesis for the TCR predilection for MHC ligands has been the consistent diagonal engagement of the MHC by the TCR. However, this orientation may be imposed by CD4 or CD8 binding to TCRs and MHC rather than by conserved structural features of the TCR (Mazza and Malissen, 2007; van Laethem et al., 2007). Analysis of our and other structures supports the idea that of a structural imposition of this geometry of engagement. In the TCR-MHC structures that contain V $\alpha$  CDR1 29Y or V $\alpha$  CDR1 27S and 30D and V $\beta$  CDR2 48Y and 54E, the sites of interaction on the MHC  $\alpha$  and  $\beta$  chains are similar and conserved in mouse and human MHC II molecules. They lie to one side of the central TCR docking axis (Figure S2). Given that V $\alpha$  CDR2 and V $\beta$  CDR1 residues will lie on the other side of this

axis, and that some residues in these regions may also have been evolutionarily selected to react with MHC, the diagonal docking mode of TCR on MHC is likely to be determined, at least in part, by the binding of evolutionarily conserved residues in V region CDRs with their target sites on MHC.

#### Are the Evolutionarily Conserved Residues in the YAe TCR Important for T Cell Activation?

Mutational studies of IA<sup>b</sup>-3K suggested that the TCR amino acids identified as binding MHC in the structural studies reported here were functionally important for IA<sup>b</sup>-3K binding to TCR (Figure 2 and Huseby et al. [2003]). However, the evolutionary hypothesis proposed here suggests that mutations in these TCR residues would often affect interaction between the TCR and MHC, regardless of the MHC target. The YAe62 TCR reacts with IA<sup>b</sup>-3K, as well as a number of allogeneic MHCs, and therefore allowed a test of the evolutionary prediction.

Retroviruses coding for the YAe62 TCR  $\alpha$  and  $\beta$  chains, expressing the wild-type sequence or with  $\alpha$ 29Y,  $\beta$ 48Y, or  $\beta$ 54E mutated to A, were created and cotransduced into a TCR-deficient hybridoma with the appropriate wild-type partner chain. Staining experiments showed that all combinations were expressed at comparable levels on the surface of the transduced cells (data not shown). The transductants were tested for their ability to react with various targets. Transductants expressing only the YAe62 TCR $\alpha$  did not respond to any target. Transductants expressing the wild-type YAe62 TCR  $\alpha\beta$  pair had allogeneic-MHC specificities characteristic of the original YAe62 hybridoma, for cells bearing only IA<sup>b</sup>-3K and for spleen cells bearing H-2<sup>b</sup>, H-2<sup>k</sup>, H-2<sup>q</sup>, H-2<sup>f</sup>, and H-2<sup>s</sup> plus endogenous mouse peptides (Huseby et al., 2005). The results are presented in Figure 6.

All three of the mutations studied severely reduced response to IA<sup>b</sup>-3K, as predicted by the structure of YAe62 bound to this ligand. The effect of the individual mutations on the response to allo-MHC depended upon the particular MHC allele. Change

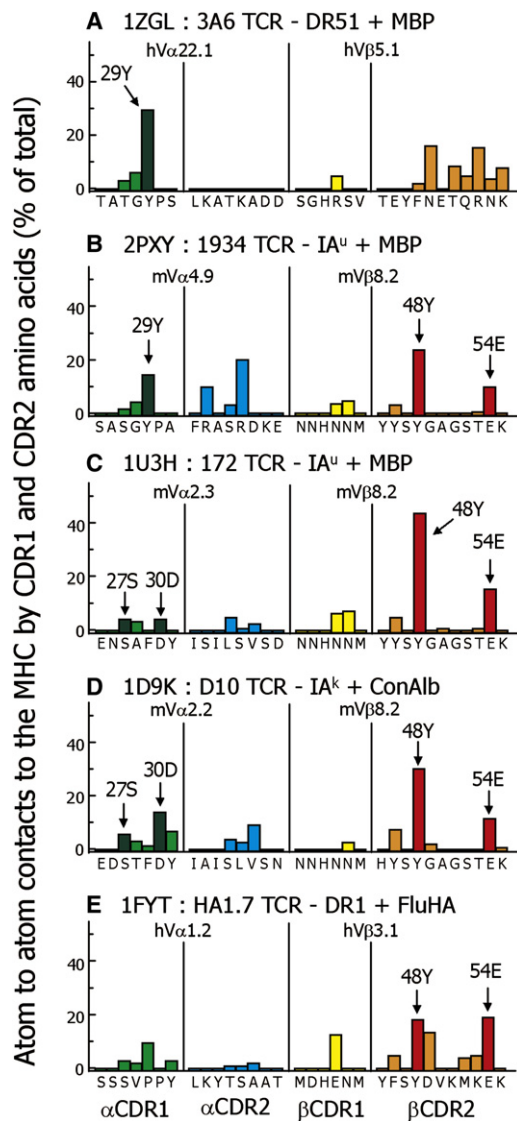


**Figure 5. Variable but Frequent Use of V $\alpha$  29Y and V $\beta$  48Y and 54E in Other TCR-MHC II Complexes**

The CDR1-CDR2 contact data for five published TCR-MHC II complex structures involving V $\alpha$  29Y or 27S-30D and/or V $\beta$  48Y and 54E were calculated, labeled, presented, and colored as in Figure 3. Items in panels are represented as follows: (A) TCR: 3A6, ligand: HLA-DR51 + peptide from myelin basic protein (MBP), and PDB: 1ZGL (Li et al., 2005); (B) TCR- 1934, ligand -mouse IA<sup>u</sup> + peptide from MBP; and PDB: 2PXY (Feng et al., 2007); (C) TCR: 172, ligand, mouse IA<sup>u</sup> + peptide from MBP; and PDB: 1U3H (Maynard et al., 2005); (D) TCR: D10, ligand: IA<sup>k</sup> + peptide from hen conalbumin (ConAlb), and PDB: 1D9K (Reinherz et al., 1999); and (E) TCR: HA-1.7, ligand: HLA-DR1 + peptide from influenza hemagglutinin (Flu-HA), and PDB: 1FYT (Hennecke et al., 2000).

of the  $\beta$ 48Y to A obliterated the ability of the TCR to react with any allo-MHC target tested. Alteration of  $\beta$ 54E to A affected all reactivities except those against H-2<sup>b</sup> and H-2<sup>s</sup>. Mutation of  $\alpha$ 29Y to A reduced the reactivity to H-2<sup>s</sup> by approximately two orders of magnitude but had no effect on the other allo-MHC reactivities. The effects of this V $\alpha$ 29Y mutation may have been less dramatic because the YAE62 TCR is strongly tilted toward the IA<sup>b</sup>  $\alpha$ 1 helix in the IA<sup>b</sup>-3K structure, and this may apply also to its

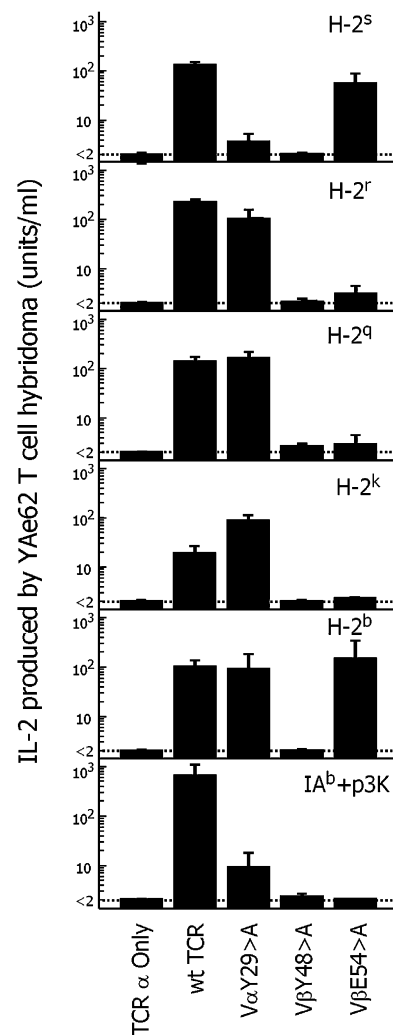


**Figure 6. The Evolutionarily Conserved, MHC-Binding Amino Acids Affect TCR Reaction with Self- and Allo-MHC**

T cell hybridomas were constructed to express the wild-type YAE62 TCR, the YAE62 TCR with CDR1 $\alpha$ 29Y mutated to A, or CDR2 $\beta$ 48Y or 54E mutated to A. All hybridomas expressed equivalent levels of TCR. The hybridomas were tested for their response to fibroblasts expressing B7, ICAM-1, and IA<sup>b</sup>-3K or to spleen cells expressing the indicated H-2 alleles bound to mouse peptides. Responses were measured with an HT-2 assay, as units/ml of IL-2 produced. Results shown are the averages and standard errors of three independent experiments. The limit of detection in the assays (dotted line) was 2 units/ml of IL-2.

reactions with allo-MHC-mouse peptides. Because, when responding to allogeneic MHC, TCRs are reacting with both foreign MHC and different arrays of peptides bound to these MHC proteins, it is possible that in responses to some allo-MHC, the loss of binding contribution by mutation of V $\alpha$ 29Y or V $\beta$ 54E can be compensated for by a particular peptide, engaged in the right configuration, by that allo-MHC protein.

Overall, these mutational results show that the amino acids we have identified as frequent contributors to MHC reaction, particularly those in V $\beta$ , operate also in reactions between the same TCR and other MHC ligands.

## DISCUSSION

Some reports support the idea that TCRs have been selected evolutionarily to react with MHC. For example, TCRs that have not been positively selected are still quite likely to react with MHC, at frequencies of  $\sim 20\%$ , and random combinations of TCR  $\alpha$  and  $\beta$  chains are also unexpectedly likely to bind MHCs (Blackman et al., 1986; Merckenschlager et al., 1997; Zerrahn et al., 1997). If evolutionary selection has occurred, it probably applies to the TCR V regions, rather than their D or J sequences, because the CDR1-CDR2 loops of the V regions are not subject to the extensive somatic variation that is introduced into the V(D)J junctional regions of CDR3. Indeed, some versions of CDR3 sequences may allow TCRs to bind ligands that do not include MHC at all (Siliciano et al., 1985; van Laethem et al., 2007).

When the first TCR and MHC-peptide complexes were solved, it was gratifying to see that the V region CDR1 and CDR2s often interacted with the MHC helices, but it was puzzling to find so much flexibility in the orientation and pitch of the TCR on the MHC (Garboczi et al., 1996; Garcia et al., 1996) (reviewed in Rudolph et al. [2006]). Clearly, universally conserved pairwise TCR-MHC contacts did not exist. However, as the number of TCR-MHC structures has increased, some consistent interactions, for particular sets of related V regions, are becoming apparent, suggesting that over evolutionary time, individual sets of V regions may have accumulated different amino acids in their CDR1-CDR2 regions to guide them toward MHC recognition.

The most complete set of data now exists for the mouse V $\beta 8$  family and related V $\beta$ s in humans. Garcia and his colleagues have concentrated on these V $\beta$ s and have pointed out the repeated similar use of V $\beta$  CDR2 46Y, 48Y, and 54E to contact MHC I and MHC II (Feng et al., 2007; Maynard et al., 2005). They have suggested that these amino acids fit very well the criteria for amino acids that have been selected evolutionarily to react with MHC.

Approaching the question from a very different direction, we predicted the existence of conserved V CDR1 and CDR2 interactions with MHC on the basis of the high frequency of broadly MHC reactive T cells in mice with limited thymic negative selection (Huseby et al., 2005; Ignatowicz et al., 1996). We reasoned that, because TCRs that reacted very well with MHC had not been eliminated in these mice, these TCRs would manifest the evolutionarily conserved reactions of TCRs with MHC better than conventional T cells.

The structures of TCRs bound to IA<sup>b</sup>-3K reported here support this notion. We studied three TCRs, one from normal mice and highly specific for MHC and peptide and two from MHC-single-peptide mice: one peptide specific, but broadly allo-MHC reactive, and another extremely peptide and MHC crossreactive. All three TCRs contained members of the V $\beta 8$  family. Two used related members of the V $\alpha 4$  family. In all three, the previously noted V $\beta 8$  interactions with the IA  $\alpha$  chain were present, especially those involving V $\beta$  48Y and 54E. For the two TCRs containing V $\alpha 4$  family members, V $\alpha$  CDR1 29Y made very similar interactions with the IA<sup>b</sup>  $\beta$  chain helix. Furthermore, these interactions are present in two other published structures using related V $\alpha$  elements, one from mouse and one from human. Finally, the data suggest that TCR V $\alpha$  regions that do not contain a 29Y

use other amino acids in a consistent way to bind MHC. In the cases described here, this is exemplified by V $\alpha$  27S and 30D in V $\alpha$ s related to mouse V $\alpha 2$ . By extension, presumably other substitutions, involving other amino acids, will apply to other V $\alpha$ s and V $\beta$ s not related to the mouse V $\beta 8$ s.

Most importantly, when comparing the combination of our and the published structures, we found that the relative contribution of V $\beta$  48Y and 54E as well as V $\alpha$  29Y was greatest for the most crossreactive T cell and least for the most conventional T cells. This observation supports our view that broad crossreactivity associated with the escape from negative selection is the hallmark of the enhanced use of conserved MHC-interacting features of TCR CDR1 and CDR2 loops. Also relative to our hypothesis, it may be noteworthy that the list of published TCRs available for this analysis does not contain many conventional MHC-II-peptide-reactive T cells, in that they are mostly from either broadly allo-MHC reactive (D10) or autoimmune T cell (3A6, 1934, and 172 [Feng et al., 2007; Li et al., 2005; Maynard et al., 2005]). We suggest that this may be why the conserved amino acid interactions were somewhat more predominant with these TCRs than with the more conventional T cells, such as B3K506 and HA1.7.

One of the questions left unanswered in our previous studies of highly crossreactive T cells was how can these T cells maintain affinity for their ligand, yet remain insensitive to many mutations in the MHC and peptide? The structural answer to this question for the YAe62 TCR is that it uses a considerably smaller, much more hydrophobic interface with the ligand than seen with conventional TCRs. This allows the TCR to ignore many mutations but maintain affinity through energy gained from the hydrophobic effect. Because our IA<sup>b</sup>-3K mutational data for many other crossreactive TCRs are very similar to that obtained for YAe62, it seems likely that this may be a common explanation for high-affinity, broadly crossreactive T cells.

Relevant to this point, it is interesting that tyrosines are emerging as perhaps one of the commonly used amino acids for conserved interaction. Because of their extended hydrophobic surface, tyrosines are particularly well suited to convert an area of weak VDW contacts into a stronger hydrophobic interaction. Furthermore, because this type of interaction is distance, but not particularly geometry, dependent, its strength may be easier to fine tune, and it may allow some flexibility for accommodating the variability in pitch and orientation seen with different TCRs. This ability to shift without losing contact may be particularly important for MHC I interaction, during which in the published structures thus far V $\beta$  48Y interacts extensively with the  $\alpha 1$  helix, but not nearly in such a fixed position as in the MHC II complexes (Buslepp et al., 2003; Colf et al., 2007).

There are not enough structures to make as strong a case for conserved amino acids in other sets of V $\alpha$  and V $\beta$  elements. However, it is worth noting that MHC II  $\beta$  chain amino acids 76, 77, and 81, the site of V $\alpha$  29Y interaction, are invariably at the site of V $\alpha$  CDR1 interaction with MHC II for TCRs using other V $\alpha$  elements. Also, MHC II  $\alpha$  chain amino acid 57, 60, and 61, the site of V $\beta$  48Y and 54E interaction, are nearly always involved in CDR2 interaction with MHC II for TCRs using other V $\beta$  elements. Similarly positioned conserved sites on MHC I molecules are often involved in other V $\alpha$  CDR1 and V $\beta$  CDR2 engagements (Marrack et al., 2008). It seems likely that conserved amino acids

within the CDR1 and CDR2 loops of these other V elements will emerge eventually from the structural data. Our hypothesis predicts that, for normal T cells, in any given complex some of these conserved features may be weakened because of the requirements imposed for negative-selection survival. Therefore, a population of T cells that have not undergone complete negative selection may again be the best place to look for these features for these other V elements.

## EXPERIMENTAL PROCEDURES

### Protein Expression and Purification

Soluble IA<sup>b</sup>-3K was produced as previously described in baculovirus-infected insect cells (Liu et al., 2002). DNA fragments encoding the V $\alpha$  and V $\beta$  portions of the mouse YAE62 and B3K506 TCRs (Huseby et al., 2005) were cloned into variants of a previously reported expression vector (Tynan et al., 2007) kindly provided by Dr. J. McCluskey and Dr. J. Rossjohn) fused to human C $\alpha$  and C $\beta$ , respectively. We used the completed and sequenced constructs to transform the Rosetta 2 strain of *E. coli* (Novagen). Functional, soluble TCR was produced as previously described (Clements et al., 2002) by refolding mixtures of denatured  $\alpha$  and  $\beta$  chains isolated from inclusion bodies made in the transformed bacteria. The refolded TCRs were further purified by the combination of FPLC size exclusion and ion-exchange chromatography. A soluble form of the 2W20 TCR, with mouse C $\alpha$  and C $\beta$ , was produced in baculovirus-infected insect cells as previously described (Huseby et al., 2005). We tested all three TCRs by surface-plasmon resonance for binding to IA<sup>b</sup>-3K to assure functionality (Huseby et al., 2006). The sequences of the V region portions of all of the constructs are shown in Figure S1.

### Crystal Production and Data Collection

Prior to the crystallization trials, we obtained noncovalent complexes of TCR-MHC-peptide complexes by mixing the proteins at equimolar concentrations. Crystallization was performed by the hanging-drop vapor-diffusion method at room temperature. The complex of the B3K506 TCR with IA<sup>b</sup>-3K was crystallized by mixing 0.5  $\mu$ l of complex solution at a concentration of 10 mg/ml with an equal volume of reservoir solution containing 17% PEG4000, 100 mM sodium citrate, and 100 mM sodium cacodylate (pH 5.1). The 2W20 TCR complex with IA<sup>b</sup>-3K was crystallized in 16% PEG4000, 100 mM calcium acetate, and 100 mM sodium cacodylate (pH 6.0). The crystals were harvested after 2 months. Crystals of the YAE62 TCR complexed with IA<sup>b</sup>-3K were obtained in 15% PEG4000, 10% glycerol, 100 mM ammonium citrate, and 100 mM sodium cacodylate (pH 5.7). Crystals normally formed within 2 weeks.

X-ray diffraction data were collected under liquid-nitrogen cryo-conditions at 100°K. Several data sets of B3K506 bound to IA<sup>b</sup>-3K, YAE62-IA<sup>b</sup>-3K, and 2W20-IA<sup>b</sup>-3K complexes were collected at ID22, SBC ID19, APS, and BL8.2.2, BL4.2.2, ALS. B3K506-IA<sup>b</sup>-3K and 2W20-IA<sup>b</sup>-3K crystals were flash-cooled in liquid nitrogen after a flash-soak in a cryoprotection solution consisting of the reservoir solution with a higher concentration of PEG4000 (35% [w/v]), and we froze YAE62-IA<sup>b</sup>-3K crystals by directly dipping the crystals into liquid nitrogen. The data were indexed, integrated, scaled, and merged with HKL2000 (Otwinowski and Minor, 1997). The B3K506-IA<sup>b</sup>-3K crystal belonged to the monoclinic space group P2<sub>1</sub> with two complexes in the asymmetric unit. The crystals of YAE62-IA<sup>b</sup>-3K and 2W20-IA<sup>b</sup>-3K belonged to the orthorhombic space group P2<sub>1</sub>2<sub>1</sub>2<sub>1</sub> with two complexes in the asymmetric unit. The statistics of for crystallographic data are summarized in Table S1.

### Structure Determination

The structures of B3K506 TCR-IA<sup>b</sup>-3K and YAE62 TCR-IA<sup>b</sup>-3K complexes were determined by molecular replacement with AmoRe (Navaraza, 1994) and Phaser (McCoy et al., 2005) with the SB27 TCR (PDB 2AK4) and IA<sup>b</sup>-3K (PDB 1LNU) as search models, respectively. 2W20 TCR-IA<sup>b</sup>-3K structure was solved by molecular replacement method that used YAE62 TCR-IA<sup>b</sup>-3K as the search model. For all three structures, there were two TCR-IA<sup>b</sup>-3K complexes per asymmetric unit. After an initial round of rigid-body refinement, the models were inspected and manually fitted with program O (Jones and Kjeldgaard, 1997; Kleywegt et al., 2001). The models were then subjected to several

rounds of alternating simulated annealing-positional refinement in CNS (Brunger et al., 1998) and then B factor refinement in CNS. Model building was performed with program O. We routinely used simulated annealing omit maps to remove the model bias. All models have good stereochemistry, as determined by the program Procheck (Laskowski et al., 1993). The statistics for the structures are summarized in Table S1, and representative electron density data for the structures are shown in Figure S3.

### Structure Analysis

For analysis, one complex of the two in the asymmetric unit was chosen on the basis of the fewest V region crystal contacts. This was most important for the B3K506 structure in which extensive V region crystal contacts in one of the complexes had clearly distorted the TCR-MHC interface. Buried molecular surface areas were calculated with GRASP (probe radius 1.4 Å) (Nicholls et al., 1991). We used NCONT in CCP4 (CCP4, 1994) to analyze the contacts between the TCRs and their ligands. Atoms within 4.5 Å of each other were considered part of the interface. Contacts involving potential electron donors and acceptors (O or N) within 3.5 Å were considered potential hydrogen bonds or salt bridges. Other contacts were considered van der Waals contacts. The total list of atomic interactions is shown in Spreadsheet S1. Molecular superimpositions were performed with Swiss PDBViewer (Guex and Peitsch, 1997). Figures were created with WebLab Veiver Pro 4.0. (Molecular Simulations).

### Nomenclature and Amino Acid Numbering

V $\beta$ s and V $\alpha$ s are named, and their amino acids are numbered according to the IUIS-Arden compilation (Arden et al., 1995; Clark et al., 1995). Mouse IA  $\alpha$  chains have a single amino acid insertion at position 10 compared to the HLA-DR and mouse IE  $\alpha$  chain. However, DR $\alpha$ -E $\alpha$  numbering is used here for consistency with previous papers.

### Analysis of the Function of TCRs Mutated in V Region Amino Acids

TCR mutants were constructed with PCR with overlapping primers and cloned into engineered restriction sites. TCR $\alpha$  constructs were cloned in MSCV-based retroviral plasmids with an IRES plus GFP as a reporter (Persons et al., 1997). TCR $\beta$  constructs were cloned in MSCV-based retroviral plasmids with an IRES plus human nerve growth-factor receptor (Pearce et al., 2003) or GFP as a reporter.

TCR constructs in retroviral plasmids were cotransfected into Phoenix cells with pCLEco accessory plasmid with Lipofectamine 2000 (Invitrogen) according to the manufacturer's instructions. We harvested retrovirus-containing supernatants 48 hr after transfection and centrifuged them to remove cell debris. All TCR constructs were expressed by retroviral transduction in 5KC-73.8.20, a T cell hybridoma that lacks endogenous TCR $\alpha$  and  $\beta$  chains (White et al., 1993). A total of 10<sup>5</sup> hybridoma T cells were spin-infected with retroviral supernatants containing 8  $\mu$ g/ml polybrene for 90 min at 37°C. Mutant TCR $\alpha$  or TCR $\beta$  chains were coexpressed with the appropriate wild-type partner. Cells were sorted (MoFlo, Dakocytomation) for equivalent expression of TCR and CD4. Responses were assessed by IL-2 production in response to fibroblasts bearing IAb-3K and B7 and ICAM-1 or spleen cells bearing allo-MHC (Huseby et al., 2006; Huseby et al., 2005).

### ACCESSION NUMBERS

The coordinates for the B3K506, 2W20, and YAE62 TCR bound to IA<sup>b</sup>-3K have been deposited in the PDB with accession numbers 3C5Z, 3C6O, and 3C6L, respectively.

### SUPPLEMENTAL DATA

Three figures, one table, and one spreadsheet are available at <http://www.immunity.com/cgi/content/full/28/3/324/DC1/>.

### ACKNOWLEDGMENTS

We thank J. White, R. Fruge, E. Kushnir and C. Brown for technical assistance, A. Fu and S. Ginell at the APS and C. Ralston and J. Nix at the ALS for

assistance in X-ray data collection, and R. Anselment and A. Marris in the NJMRC. We appreciate helpful input from L. Gapin at NJMRC and C. Garcia at Stanford University. This work was supported in part by USPHS grants AI-17134, AI-18785, and AI-22295 and donations from Alan LaPorte and the Zuckerman Family to the X-ray facility at NJMRC. W.A.M. was supported by the Australian NHMRC, Victoria State Government, and Monash University.

Received: January 8, 2008

Accepted: January 15, 2008

Published online: February 28, 2008

## REFERENCES

- Arden, B., Clark, S.P., Kabelitz, D., and Mak, T.W. (1995). Mouse T-cell receptor variable gene segment families. *Immunogenetics* **42**, 501–530.
- Blackman, M., Yague, J., Kubo, R., Gay, D., Coleclough, C., Palmer, E., Kappler, J., and Marrack, P. (1986). The T cell repertoire may be biased in favor of MHC recognition. *Cell* **47**, 349–357.
- Bluthmann, H., Kisielow, P., Uematsu, Y., Malissen, M., Krimpenfort, P., Berns, A., von Boehmer, H., and Steinmetz, M. (1988). T-cell-specific deletion of T-cell receptor transgenes allows functional rearrangement of endogenous alpha- and beta-genes. *Nature* **334**, 156–159.
- Brunger, A.T., Adams, P.D., Clore, G.M., DeLano, W.L., Gros, P., Grosse-Kunstleve, R.W., Jiang, J.S., Kuszewski, J., Nilges, M., Pannu, N.S., et al. (1998). Crystallography & NMR system: A new software suite for macromolecular structure determination. *Acta Crystallogr. D Biol. Crystallogr.* **54**, 905–921.
- Buslepp, J., Wang, H., Biddison, W.E., Appella, E., and Collins, E.J. (2003). A correlation between TCR Valpha docking on MHC and CD8 dependence: Implications for T cell selection. *Immunity* **19**, 595–606.
- Clark, S.P., Arden, B., Kabelitz, D., and Mak, T.W. (1995). Comparison of human and mouse T-cell receptor variable gene segment subfamilies. *Immunogenetics* **42**, 531–540.
- Clements, C.S., Kjer-Nielsen, L., MacDonald, W.A., Brooks, A.G., Purcell, A.W., McCluskey, J., and Rossjohn, J. (2002). The production, purification and crystallization of a soluble heterodimeric form of a highly selected T-cell receptor in its unliganded and liganded state. *Acta Crystallogr. D Biol. Crystallogr.* **58**, 2131–2134.
- Colf, L.A., Bankovich, A.J., Hanick, N.A., Bowerman, N.A., Jones, L.L., Kranz, D.M., and Garcia, K.C. (2007). How a single T cell receptor recognizes both self and foreign MHC. *Cell* **129**, 135–146.
- CCP4 (Collaborative Computational Project, Number 4) (1994). The CCP4 suite: Programs for protein crystallography. *Acta Crystallogr. D Biol. Crystallogr.* **50**, 760–763.
- Feng, D., Bond, C.J., Ely, L.K., Maynard, J., and Garcia, K.C. (2007). Structural evidence for a germline-encoded T cell receptor-major histocompatibility complex interaction 'codon'. *Nat. Immunol.* **8**, 975–983.
- Fung-Leung, W.P., Surh, C.D., Liljedahl, M., Pang, J., Leturcq, D., Peterson, P.A., Webb, S.R., and Karlsson, L. (1996). Antigen presentation and T cell development in H2-M-deficient mice. *Science* **271**, 1278–1281.
- Garboczi, D.N., Ghosh, P., Utz, U., Fan, Q.R., Biddison, W.E., and Wiley, D.C. (1996). Structure of the complex between human T-cell receptor, viral peptide and HLA-A2. *Nature* **384**, 134–141.
- Garcia, K.C., Degano, M., Stanfield, R.L., Brunmark, A., Jackson, M.R., Peterson, P.A., Teyton, L., and Wilson, I.A. (1996). An alphabeta T cell receptor structure at 2.5 Å and its orientation in the TCR-MHC complex. *Science* **274**, 209–219.
- Guex, N., and Peitsch, M.C. (1997). SWISS-MODEL and the Swiss-PdbViewer: An environment for comparative protein modeling. *Electrophoresis* **18**, 2714–2723.
- Hennecke, J., Carfi, A., and Wiley, D.C. (2000). Structure of a covalently stabilized complex of a human alphabeta T-cell receptor, influenza HA peptide and MHC class II molecule, HLA-DR1. *EMBO J.* **19**, 5611–5624.
- Hogquist, K.A., Jameson, S.C., Heath, W.R., Howard, J.L., Bevan, M.J., and Carbone, F.R. (1994). T cell receptor antagonist peptides induce positive selection. *Cell* **76**, 17–27.
- Huseby, E.S., Crawford, F., White, J., Kappler, J., and Marrack, P. (2003). Negative selection imparts peptide specificity to the mature T cell repertoire. *Proc. Natl. Acad. Sci. USA* **100**, 11565–11570.
- Huseby, E.S., Crawford, F., White, J., Marrack, P., and Kappler, J.W. (2006). Interface-disrupting amino acids establish specificity between T cell receptors and complexes of major histocompatibility complex and peptide. *Nat. Immunol.* **7**, 1191–1199.
- Huseby, E.S., White, J., Crawford, F., Vass, T., Becker, D., Pinilla, C., Marrack, P., and Kappler, J.W. (2005). How the T cell repertoire becomes peptide and MHC specific. *Cell* **122**, 247–260.
- Ignatowicz, L., Kappler, J., and Marrack, P. (1996). The repertoire of T cells shaped by a single MHC/peptide ligand. *Cell* **84**, 521–529.
- Jerne, N.K. (1971). The somatic generation of immune recognition. *Eur. J. Immunol.* **1**, 1–9.
- Jones, T.A., and Kjeldgaard, M. (1997). Electron-density map interpretation. *Methods Enzymol.* **277**, 173–207.
- Kappler, J.W., Roehm, N., and Marrack, P. (1987). T cell tolerance by clonal elimination in the thymus. *Cell* **49**, 273–280.
- Kleywegt, G.J., Zou, J.Y., Kjeldgaard, M., and Jones, T.A. (2001). Around O. In *International Tables for Crystallography. Crystallography of Biological Macromolecules* (Dordrecht, The Netherlands: Kluwer Academic Publishers), pp. 353–367.
- Laskowski, R., MacArthur, M., Moss, D., and Thornton, J. (1993). PROCHECK: A program to check the stereochemical quality of protein structures. *J. Appl. Cryst.* **26**, 283–291.
- Lefranc, M.P., Pommie, C., Ruiz, M., Giudicelli, V., Foulquier, E., Truong, L., Thouvenin-Contet, V., and Lefranc, G. (2003). IMGT unique numbering for immunoglobulin and T cell receptor variable domains and Ig superfamily V-like domains. *Dev. Comp. Immunol.* **27**, 55–77.
- Li, Y., Huang, Y., Lue, J., Quandt, J.A., Martin, R., and Mariuzza, R.A. (2005). Structure of a human autoimmune TCR bound to a myelin basic protein self-peptide and a multiple sclerosis-associated MHC class II molecule. *EMBO J.* **24**, 2968–2979.
- Liu, X., Dai, S., Crawford, F., Fruge, R., Marrack, P., and Kappler, J. (2002). Alternate interactions define the binding of peptides to the MHC molecule IA(b). *Proc. Natl. Acad. Sci. USA* **99**, 8820–8825.
- Marrack, P., Scott-Browne, J.P., Dai, S., Gapin, L., and Kappler, J.W. (2008). Evolutionarily conserved amino acids in TCR V regions and MHC control their interaction. *Annu. Rev. Immunol.* in press. Published online January 22, 2008. 10.1146/annurev.immunol.26.021607.090421.
- Martin, W.D., Hicks, G.G., Mendiratta, S.K., Leva, H.I., Ruley, H.E., and Van Kaer, L. (1996). H2-M mutant mice are defective in the peptide loading of class II molecules, antigen presentation, and T cell repertoire selection. *Cell* **84**, 543–550.
- Maynard, J., Petersson, K., Wilson, D.H., Adams, E.J., Blondelle, S.E., Boulangier, M.J., Wilson, D.B., and Garcia, K.C. (2005). Structure of an autoimmune T cell receptor complexed with class II peptide-MHC: Insights into MHC bias and antigen specificity. *Immunity* **22**, 81–92.
- Mazza, C., and Malissen, B. (2007). What guides MHC-restricted TCR recognition? *Semin. Immunol.* **19**, 225–235.
- McCoy, A.J., Grosse-Kunstleve, R.W., Storoni, L.C., and Read, R.J. (2005). Likelihood-enhanced fast translation functions. *Acta Crystallogr. D Biol. Crystallogr.* **61**, 458–464.
- Merkenschlager, M., Graf, D., Lovatt, M., Bommhardt, U., Zamoyska, R., and Fisher, A.G. (1997). How many thymocytes audition for selection? *J. Exp. Med.* **186**, 1149–1158.
- Miyazaki, T., Wolf, P., Tourne, S., Waltzinger, C., Dierich, A., Barois, N., Ploegh, H., Benoist, C., and Mathis, D. (1996). Mice lacking H2-M complexes, enigmatic elements of the MHC class II peptide-loading pathway. *Cell* **84**, 531–541.
- Navaraza, J. (1994). AMoRe: An automated package for molecular replacement. *Acta Crystallogr. A* **50**, 157–163.

- Nicholls, A., Sharp, K.A., and Honig, B. (1991). Protein folding and association: Insights from the interfacial and thermodynamic properties of hydrocarbons. *Proteins Struct. Funct. Genet.* *11*, 281–296.
- Otwinowski, Z., and Minor, W. (1997). Processing of X-ray diffraction data collected in oscillation mode. In *Macromolecular Crystallography Part A*, J.C.W. Carter and R.M. Sweet, eds. (New York: Academic Press), pp. 307–326.
- Pearce, E.L., Mullen, A.C., Martins, G.A., Krawczyk, C.M., Hutchins, A.S., Zeddiak, V.P., Banica, M., DiCioccio, C.B., Gross, D.A., Mao, C.A., et al. (2003). Control of effector CD8+ T cell function by the transcription factor Eomesodermin. *Science* *302*, 1041–1043.
- Persons, D.A., Allay, J.A., Allay, E.R., Smeyne, R.J., Ashmun, R.A., Sorrentino, B.P., and Nienhuis, A.W. (1997). Retroviral-mediated transfer of the green fluorescent protein gene into murine hematopoietic cells facilitates scoring and selection of transduced progenitors in vitro and identification of genetically modified cells in vivo. *Blood* *90*, 1777–1786.
- Rees, W., Bender, J., Teague, T.K., Kedl, R.M., Crawford, F., Marrack, P., and Kappler, J. (1999). An inverse relationship between T cell receptor affinity and antigen dose during CD4(+) T cell responses in vivo and in vitro. *Proc. Natl. Acad. Sci. USA* *96*, 9781–9786.
- Reinherz, E.L., Tan, K., Tang, L., Kern, P., Liu, J., Xiong, Y., Hussey, R.E., Smolyar, A., Hare, B., Zhang, R., et al. (1999). The crystal structure of a T cell receptor in complex with peptide and MHC class II. *Science* *286*, 1913–1921.
- Rudolph, M.G., Stanfield, R.L., and Wilson, I.A. (2006). How TCRs bind MHCs, peptides, and coreceptors. *Annu. Rev. Immunol.* *24*, 419–466.
- Sebzda, E., Wallace, V.A., Mayer, J., Yeung, R.S., Mak, T.W., and Ohashi, P.S. (1994). Positive and negative thymocyte selection induced by different concentrations of a single peptide. *Science* *263*, 1615–1618.
- Siliciano, R.F., Keegan, A.D., Dintzis, R.Z., Dintzis, H.M., and Shin, H.S. (1985). The interaction of nominal antigen with T cell antigen receptors. I. Specific binding of multivalent nominal antigen to cytolytic T cell clones. *J. Immunol.* *135*, 906–914.
- Sprent, J., Lo, D., Gao, E.K., and Ron, Y. (1988). T cell selection in the thymus. *Immunol. Rev.* *101*, 173–190.
- Tynan, F.E., Reid, H.H., Kjer-Nielsen, L., Miles, J.J., Wilce, M.C., Kostenko, L., Borg, N.A., Williamson, N.A., Beddoe, T., Purcell, A.W., et al. (2007). A T cell receptor flattens a bulged antigenic peptide presented by a major histocompatibility complex class I molecule. *Nat. Immunol.* *8*, 268–276.
- van Laethem, F., Sarafova, S.D., Park, J.-H., Tai, X., Pobeziński, L., Guinter, T.I., Adoro, A., Adams, A., Sharrow, S.O., Feigenbaum, L., and Singer, A. (2007). Deletion of CD4 and CD8 coreceptors permits generation of  $\alpha\beta$ T cells that recognize antigens independently of the MHC. *Immunity* *27*, 735–750.
- White, J., Pullen, A., Choi, K., Marrack, P., and Kappler, J.W. (1993). Antigen recognition properties of mutant V beta 3+ T cell receptors are consistent with an immunoglobulin-like structure for the receptor. *J. Exp. Med.* *177*, 119–125.
- Zerrahn, J., Held, W., and Raulet, D.H. (1997). The MHC reactivity of the T cell repertoire prior to positive and negative selection. *Cell* *88*, 627–636.